Solid State Communications, Vol. 15, pp. 59–63, 1974. Pergamon Press. Printed in Great Britain

REFRACTIVE INDEX OF $Ga_{1-x}Al_xAs$

Martin A. Afromowitz

Bell Laboratories, Murray Hill, New Jersey, U.S.A.

(*Received* 18 *February* 1974 *by J. Tauc*)

A semi-empirical method for calculating the room temperature refractive index of $Ga_{1-x}Al_xAs$ at energies below the direct band edge is presented. This quantity is important in the design of GaAs heterostructure lasers as well as other wave-guiding devices using these materials. The calculated values compare favorably with recent data. The method is shown to be useful for the $Ga_{1-x}As_xP$ system as well.

A SEMI-EMPIRICAL method for calculating the room temperature index of refraction of $Ga_{1-x}Al_xAs$ at energies below the direct band edge is presented. This quantity is important in the design of GaAs heterostructure lasers as well as other wave-guiding devices using these materials.

The calculation of the index of refraction n of the alloy system rests largely on the single-effective-oscillator model proposed by Wemple and DiDomenico,[1] which has been shown to represent refractive index data very well for a wide variety of covalent, ionic, and amorphous[2] materials at energies sufficiently below the direct band edge. In that model, one approximates the ϵ_2 spectrum of the material with a delta function of strength $\pi E_d/2$ at an energy E_0. The dashed lines in Fig. 1 show the best fit of the single-effective-oscillator formula

$$n^2 - 1 = \frac{E_0 E_d}{E_0^2 - E^2} \qquad (1)$$

to the data for GaAs[3] and AlAs.[4] These curves give the reciprocal of the polarizability $\chi^{-1} = (n^2 - 1)^{-1}$ vs $(E/E_0)^2$, which from equation (1) is a straight line.

We note that the straight-line fit in the case of AlAs is excellent. The data for GaAs, however, depart substantially from the single-effective-oscillator curve at energies approaching the band edge. On this plot, the band edge of GaAs occurs at an abscissa value of 0.155.

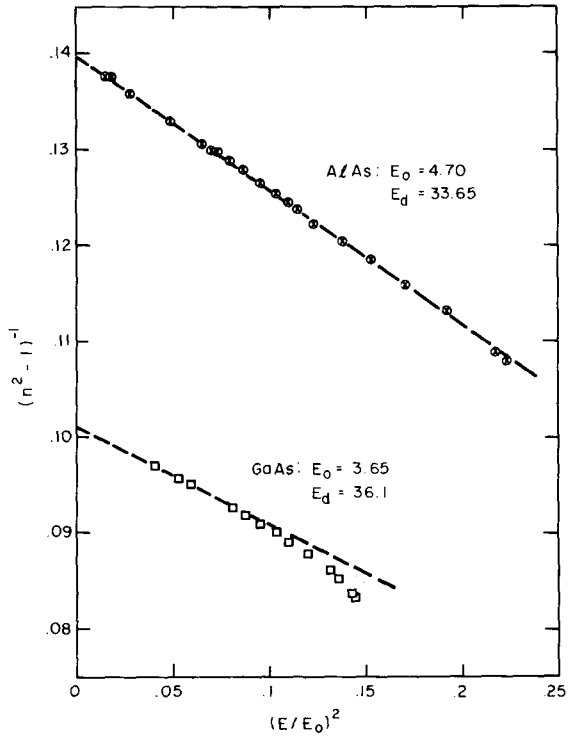

FIG. 1. Reciprocal polarizability $1/\chi = 1/(n^2 - 1)$ of GaAs and AlAs plotted vs $(E/E_0)^2$, where E is the photon energy and E_0 is the energy position parameter in the single-effective-oscillator model. Dashed lines are the best single-effective-oscillator fit to the data.

Our aim is to provide a reasonable interpolation scheme between the GaAs and AlAs alloy end points. Matters are complicated by the lack of agreement of the data for GaAs with the simple model at the band edge, which is the energy range of most interest for GaAs laser devices. A more complex model is therefore needed. We will first describe this new model which yields very close agreement with the data for GaAs. We then describe the interpolation scheme used, and compare the results of the calculation of refractive index for the GaAlAs and GaAsP alloy systems with experimental data.

One need only write an expansion of one of the Kramers–Kronig relations to see why the single-effective-oscillator model fails for energies approaching the direct gap. In particular, the real part of the dielectric constant, ϵ_1, is related to the imaginary part, ϵ_2, by the equation

$$\epsilon_1(E) - 1 = \frac{2}{\pi} P \int_0^\infty \frac{E' \epsilon_2(E') dE'}{E'^2 - E^2} \tag{2}$$

where P denotes the principal value of the integral. Considering $\epsilon_1(E)$ in the range of energies below the direct band edge, E_Γ, in which ϵ_2 may be taken as zero, we may expand equation (2) in the following form

$$\epsilon_1(E) - 1 = \chi(E) = \frac{2}{\pi} \int_{E_\Gamma}^\infty \epsilon_2(E') \left[\frac{1}{E'} + \frac{E^2}{E'^3} + \frac{E^4}{E'^5} + \dots \right] dE', \tag{3}$$

for $E < E_\Gamma \leqslant E'$.

Integrating each term separately gives a power series expansion for χ:

$$\chi(E) = M_{-1} + M_{-3}E^2 + M_{-5}E^4 + \dots \tag{4}$$

where the coefficients are moments of the ϵ_2 spectrum

$$M_i = \frac{2}{\pi} \int_{E_\Gamma}^\infty \epsilon_2(E) E^i \, dE \tag{5}$$

The higher-order moments which appear in equation (4) weight the low-energy side of the ϵ_2 spectrum. Their contribution to χ becomes significant only as E approaches E_Γ. Since the single-effective-oscillator model does not represent the low-energy range of the ϵ_2 spectrum accurately, we must expect the model to depart from the data as E approaches E_Γ.

We propose to model the ϵ_2 spectrum in a different way using an emprical form which agrees closely with the data on the low-energy side of the spectrum. This three-parameter model is as follows:

$$\epsilon_2(E) = \begin{cases} \eta E^4, & E_\Gamma \leqslant E \leqslant E_f \\ 0, & \text{otherwise} \end{cases} \tag{6}$$

Substituting this form into the moment equation (5) yields

$$M_{-1} = \frac{\eta}{2\pi}(E_f^4 - E_\Gamma^4) \tag{7}$$

$$M_{-3} = \frac{\eta}{\pi}(E_f^2 - E_\Gamma^2). \tag{8}$$

We next constrain χ calculated from this model to fit the data at low energy to order E^2. Therefore, we may expand equation (1) and get

$$\chi = \frac{E_d}{E_0} + E^2 \frac{E_d}{E_0^3} = M_{-1} + M_{-3}E^2. \tag{9}$$

Equating like terms we can express the new parameters E_f and η in terms of E_0 and E_d:

$$E_f = (2E_0^2 - E_\Gamma^2)^{\frac{1}{2}} \tag{10}$$

$$\eta = \pi E_d / 2E_0^3 (E_0^2 - E_\Gamma^2) \tag{11}$$

Using the values of E_0 and E_d derived for GaAs and AlAs (see Fig. 1) and energy gaps of 1.424[5] and 2.95[6] eV, respectively, we obtain for GaAs, $E_f = 4.962$ and $\eta = 0.1032$, and for AlAs, $E_f = 5.966$ and $\eta = 0.03803$.

Figure 2 compares the actual ϵ_2 spectrum of GaAs with that of our empirical model (dashed curve) and the single-effective-oscillator model. The important point is that the low-energy side of the ϵ_2 spectrum is given accurately by our model. This is the region which contributes most heavily to the higher order moments, which are important in predicting the index of refraction for energies approaching E_Γ. Substituting equation (6) into equation (3) yields

$$\chi(E) = M_{-1} + M_{-3}E^2 + \frac{\eta}{\pi} E^4 \times \ln[(E_f^2 - E^2)/(E_\Gamma^2 - E^2)]. \tag{12}$$

This equation reproduces the index of refraction data for GaAs[3] within 0.004 from 0.895 to 1.7 μm. The fit to to the data for AlAs[4] is within 0.004 for energies to 1.5 eV, and within 0.014 up to 2 eV. We conclude that a very good idea of the index of refraction of the alloy system could be obtained in the energy range of interest

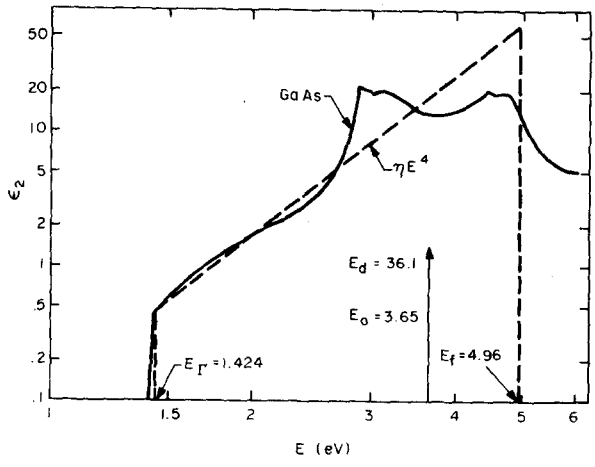

FIG. 2. Representations of the ϵ_2 spectrum of GaAs. Solid curve is calculated from data (reference 15). Delta function represents single-effective-oscillator model. Dashed curve is the empirical model used in this calculation.

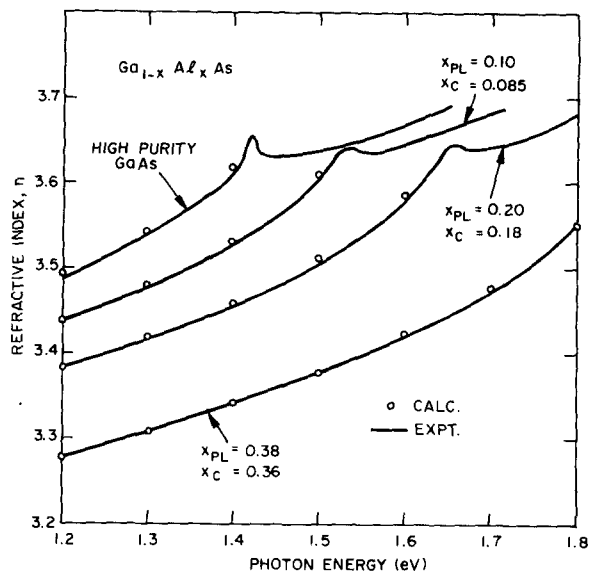

FIG. 3. Comparison of refractive index data[9] and calculated results of this model for the $Ga_{1-x}Al_xAs$ system. Solid curves represent data, and x_{PL} denotes the experimentally determined alloy composition. Circles denote calculated values based upon compositions x_c which best fit the data.

if an accurate interpolation of the parameters E_Γ, E_f and η were provided.

We propose the following interpolation scheme. It has been shown by Wemple[7] *et al.* that for the III–V compounds and the structurally similar ternary analogs, the single-effective-oscillator parameter E_0 scales linearly with the energy of the lowest direct band gap E_Γ,

$$E_0 = A + BE_\Gamma \qquad (13)$$

where $A \approx 2.6$ and $B \approx 3/4$.
Also known is the shift in the energy of the direct gap with alloy composition[8] measured by electro-reflectance,

$$E_\Gamma(x) = 1.424 + 1.266x + 0.26x^2 \qquad (14)$$

where x is the AlAs mole fraction. Combining these two equations with the values of E_0 for GaAs and AlAs gives the variation of E_0 with alloy composition. (See Appendix) The only other parameter to be interpolated is E_d, which for lack of a more perfect understanding is taken to be a linear function of the alloy composition.

A comparision of the predictions of this model with recent experimental data on the $Ga_{1-x}Al_xAs$ system[9] is shown in Fig. 3. The alloy compositions indicated on the figure as x_{PL} were estimated by measuring photoluminescence peak positions. The model presented above can reproduce the experimental curves

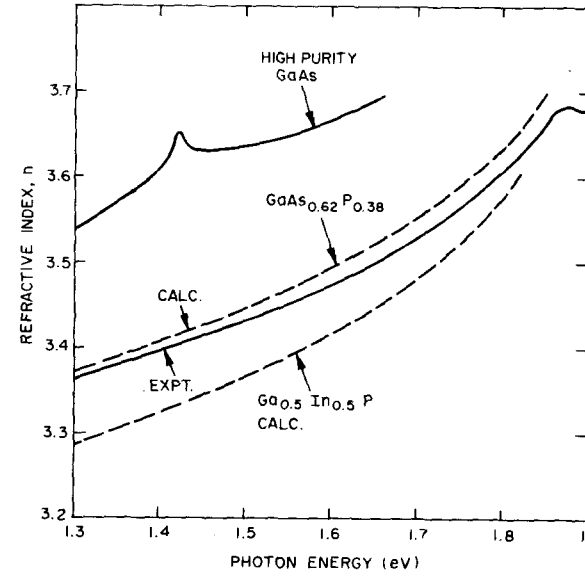

FIG. 4. Comparison fo refractive inded data[14] and calculated results for $GaAs_{0.5}In_{0.5}P$.

using slightly different composition values, labelled x_c. This discrepancy is within the range of error expected for experimental determination of alloy composition.

This model has also been applied to the $GaAs_{1-x}P_x$ and the $Ga_xIn_{1-x}P$ systems. Refractive index data for GaP[10] and InP[11] coupled with equations giving the band gap variation with alloy composition for $GaAs_{1-x}P_x$ [12] and $Ga_xIn_{1-x}P$ [13] permit the calculation of the index of refraction below the direct band gap for the full composition range of these systems as well. (See appendix) As an indication of the accuracy of this model for the $GaAs_{1-x}P_x$ system, we present data in Fig. 4 of the index of refraction of $GaAs_{0.62}P_{0.38}$ [14] as well as calculated results using this model. We also show a calculated index curve for $Ga_{0.5}In_{0.5}P$, for which system no data exists. This composition may be of special interest because of its very close lattice match to GaAs.

Acknowledgements – The author would like to thank S.H. Wemple for many useful discussions, H.C. Casey, Jr. for making his refractive index data available to me prior to publication, and D.L. Rode for helpful criticism and encouragement.

APPENDIX

In order to facilitate calculation of the index of refraction for the three systems discussed above, we present the equations for E_0, E_d and E_Γ as functions of alloy composition, to be used in conjunction with equations 7, 8, 10 11 and 12.

$Ga_{1-x}Al_xAs$:
$$E_0 = 3.65 + 0.871x + 0.179x^2$$
$$E_d = 36.1 - 2.45x$$
$$E_\Gamma = 1.424 + 1.266x + 0.26x^2$$

$GaAs_{1-x}P_x$:
$$E_0 = 3.65 + 0.721x + 0.139x^2$$
$$E_d = 36.1 + 0.35x$$
$$E_\Gamma = 1.441 + 1.091x + 0.21x^2$$

$Ga_xIn_{1-x}P$:
$$E_0 = 3.391 + 0.524x + 0.595x^2$$
$$E_d = 28.91 + 7.54x$$
$$E_\Gamma = 1.34 + 0.668x + 0.758x^2$$

REFERENCES

1. WEMPLE S.H. and DIDOMENICO M., Jr., *Phys. Rev.* B **3**, 1338 (1971).
2. WEMPLE S.H., *Phys. Rev.* B 7, 3767 (1973).
3. MARPLE D.T.F., *J. Appl. Phys.* **35**, 1241 (1964). See also data in *Semiconductors and Semi-metals*, p. 513 ff. Vol. 3, edited by WILLARDSON R.K. and BEER A.C. (Academic Press, N.Y. (1967)).
4. FERN R.E. and ONTON A., *J. Appl. Phys.* **42**, 3499 (1971).
5. SELL D.D., CASEY H.C., Jr. and WECHT K.W., *J. Appl. Phys.* **45**, 2650 (1974).
6. ONTON A., *Proc. 10th Int. Conf. Phys. Semiconductors*, Cambridge, Mass., p.107..
7. WEMPLE S.H., GABBE J.D. and BOYD G.D., to be published.
8. BEROLO O. and WOOLEY J.C., *Can. J. Phys.* **49**, 1335 (1971).
9. CASEY H.C., Jr., SELL D.D., and PANISH M., *Appl. Phys. Lett.* **24**, 63 (1974).
10. BOND W.L., *J. Appl. Phys.* **36**, 1674 (1965).
11. PETTIT G.D. and TURNER W.J., *J. Appl. Phys.* **36**, 2081 (1965).

12. THOMPSON A.G., CARDONA M., and SHAKLEE K.L., *Phys. Rev.* **146**, 601 (1966).
13. ONTON A., LORENZ M.R. and REUTER W., *J. Appl. Phys.* **42**, 3420 (1971).
14. CASEY H.C., Jr., *J. Appl. Phys.* **45**, 2766 (1974).
15. EDEN R.C., Stanford Electronics Laboratories, Stanford University, Report SEL-67-038 (1967).